ICSV13 - Vienna
The Thirteenth International Congress on Sound and Vibration
Vienna, Austria, July 2-6, 2006

INVESTIGATION OF AEROELASTIC STABILITY OF A HINGELESS ROTOR SYSTEM WITH TAILORED COMPOSITE FLEXURES

Do-Hyung Kim*, Keun-Woong Song, Seung-Ho Kim, and Gene Joo

Rotor System Department, Korea Aerospace Research Institute
45 Eoeun-dong, Yuseong-gu, Daejeon, 305-333, Korea
dhkim@kari.re.kr (e-mail address of lead author)

Abstract

For hingeless rotor system, the flap and lag hinges are removed and the flap and lag motions are realized through the elastic deformation of the flexures. Large amount of aerodynamic moments can be transmitted to rotor shaft because of the absence of hinges; accordingly aeroelastic instability problems of rotor system can occur. In order to increase aeroelastic stability, sufficient in-plane damping is required. In this study, composite tailoring technique has been applied to the flexures of a small-scaled hingeless rotor system. Composite flexures can have different coupling stiffness even though they have the same isotropic stiffness terms, and the aeroelastic characteristics can be greatly different. The effects of each coupling stiffness term on the aeroelastic stability have been investigated. Analysis results show that the in-plane damping can be changed remarkably when a torsion/flap bending coupling is changed. In addition, the application of viscoelastic damping material is considered to increase in-plane damping a little more.

INTRODUCTION

Hingeless or bearingless main rotor systems for helicopters offer fairy simple hub structures compared to conventional articulated rotor systems and the flexure component allow flap and lag motions through its elastic deformation. However, large amount of aerodynamic moments can be transmitted to rotor shaft because of the absence of hinges, accordingly aeromechanical and aeroelastic stability problems can occur. In order to increase aeroelastic stability, sufficient in-plane (lead-lag mode) damping is required. . Conventional helicopters have been equipped with elastomeric or hydraulic lag mode dampers in order to maintain stabilities. However mechanical damping devices increase complexity, weight and aerodynamic drag [1]. Therefore

practical and effective method is preferred for the stability enhancement.

For this purpose, active control approaches to reduce vibration and increase stability margin have been intensively studied. These efforts include trailing-edge flaps (TEF) with smart actuators [2], controllable twist blades with embedded piezoelectric actuators [3], stability augmentation system [4], magneto-rheological fluid damper [5], active constrained layer damping [1], and so on. Active methods can be effective at designed operating condition and show excellent performance. However additional equipments and costs are required for the construction of control system, and moreover, performance degradation can take place due to the operating condition variations, and sometimes it can induce instabilities. Compared with active control approach, passive damping enhancement approaches support baseline stability, though it does not give us outstanding performance. Among various passive approaches, the tailoring technique for composite laminate and the surface damping treatment employing viscoelastic materials [6] are well known methods to reduce vibrations in numerous dynamic applications. Composite structures can be made to have different stiffness and strength according to stacking sequences, and they can have coupling stiffness in contrast to isotropic cases. When flexures with different coupling stiffness are applied to a rotor system, even though they have the same isotropic stiffness terms, the structural dynamic and aeroelastic characteristics can be greatly different.

In this study, composite tailoring technique has been applied to composite flexures of a small-scaled hingeless rotor system. The effects of coupling stiffness of composite flexures on the aeroelastic stability of a small-scaled rotor system have been investigated. The aeroelastic stability of the rotor system with different flexures are calculated and compared. For a specific case, the effects of individual coupling stiffness on the aeroelastic stability are examined.

HINGELESS ROTOR SYSTEM

Hub System

The purpose of this study is the investigation of the effects of coupling stiffness on the aeroelastic stability of a small-scaled rotor system. In order to realize different coupling stiffness terms easily, the hub system was designed in simple configuration with flat plate-like flexures as shown in *Figure 1*.

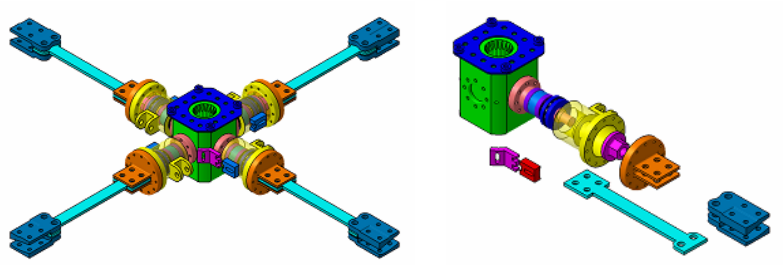

Figure 1 – Configuration of hingeless hub system

The coupling stiffness can be changed according to the stacking sequence. The hub system has four arms, pitch bearing assemblies, and flexures. The rotor blade is connected at the end of each flexure.

Composite Flexure

The flexure is flat carbon/epoxy laminate beam and the other part of hub structure is made of isotropic material. Therefore, the anisotropic stiffness is only calculated for flexure region. Although the cross-sectional analysis is coupled with the global analysis, effective sectional elastic constants including effects of general warping deformations in and out of plane are easily obtained from a linearization of governing equations about reference state (undeformed and unstressed state). The linearized form is quasi-linear because strain measures are nonlinear functions of the displacements and rotations. Considering energy equilibrium in an infinitesimal 'slice' of a loaded beam, the following governing equations can be obtained [7, 8].

$$\begin{aligned} F' + \tilde{\kappa}F + f = 0 \\ M' + (\tilde{e}_1 + \tilde{e})F + \tilde{\kappa}M + m = 0 \end{aligned} \tag{1}$$

where F and M are the cross-sectional force and moment stress vectors in the deformed beam basis, and f and m are the applied force and moment vectors about the sectional reference point. $\tilde{\kappa}$, $\tilde{e}$, and $\tilde{e}_1$ are skew-symmetric matrix of which components are the force and moment strains. Detail description is given in ref. 7. Now the cross-sectional warping is discretized as a two-dimensional shape function and finite-element equations governing the warping can be obtained.

$$\begin{aligned} JW'' - HW' - EW + L\Psi' - R\Psi = 0 \\ L^T W' + R^T W + A\Psi = Q \end{aligned} \tag{2}$$

where Q is column matrix containing F and M, and the redundancy of 6 degrees of freedom in W has been appropriately removed as discussed in ref. 8. A column matrix Ψ is defined as $\Psi = \{\bar{e}\ \bar{\kappa}\}^T$, where $\bar{e} = \{\bar{e}_{11}\ 2\bar{e}_{12}\ 2\bar{e}_{13}\}^T$ and $\bar{\kappa} = \{\kappa_1\ \kappa_2\ \kappa_3\}^T$. The matrices J, H, E, L, R and A depend on the cross-sectional configuration and property, and these can be found in ref. 7 and 8.

If f and m are taken to be zero in Eq. (1) and (2). We can obtain effective elastic sectional constants for unloaded condition as follows:

$$\begin{Bmatrix} F \\ M \end{Bmatrix} = \begin{bmatrix} A & B \\ B^T & D \end{bmatrix} \begin{Bmatrix} \bar{e} \\ \bar{\kappa} \end{Bmatrix} = [T] \begin{Bmatrix} \bar{e} \\ \bar{\kappa} \end{Bmatrix} \tag{3}$$

where A, B, and D are 3×3 matrices that depend on the material properties and the geometry of the cross section. Generally it is appropriate to neglect the shear force, so the F_y and F_z rows and columns of T^{-1} are eliminated to produce S^{-1}, and the inverse

of the resulting matrix gives S [9].

$$\begin{Bmatrix} F_x \\ M_x \\ M_y \\ M_z \end{Bmatrix} = \begin{bmatrix} S_{uu} & S_{tu} & S_{wu} & S_{vu} \\ S_{tu} & S_{tt} & S_{wt} & S_{vt} \\ S_{wu} & S_{wu} & S_{ww} & S_{vw} \\ S_{vu} & S_{vt} & S_{vw} & S_{vv} \end{bmatrix} \begin{Bmatrix} \bar{e}_{11} \\ \kappa_1 \\ \kappa_2 \\ \kappa_3 \end{Bmatrix} = [S] \begin{Bmatrix} \bar{e}_{11} \\ \kappa_1 \\ \kappa_2 \\ \kappa_3 \end{Bmatrix} \tag{4}$$

The diagonal terms of S present isotropic sectional stiffness and off-diagonal terms are coupling stiffness. The commercial code CAMRAD II (Comprehensive Analytical Model of Rotorcraft Aerodynamic and Dynamic) provide an opportunity to model the structural component as anisotropic beam using 10 independent sectional stiffness properties. In order to calculate S, cross section of the flexure was modelled as 9 rectangular elements with 8 nodes. The material properties of carbon/epoxy prepreg (HT145/RS1222, Hankuk Fiber) are as follows:

E_1 = 112.156 GPa, E_2 = 8.109 GPa, G_{12} = 4.647 GPa, ν_{12} = 0.331
ρ = 1.57 g/cm^3, ply thickness = 0.14 mm

Four types of flexures with different stacking sequence are considered in this study. Each flexure is laminated using 20 plies and the dimension of the flexure is shown in *Figure 2*. The calculated sectional stiffness values in center region are presented in *Table 1*. We can see that case A1 and A2 have different coupling stiffness although they have the same diagonal terms.

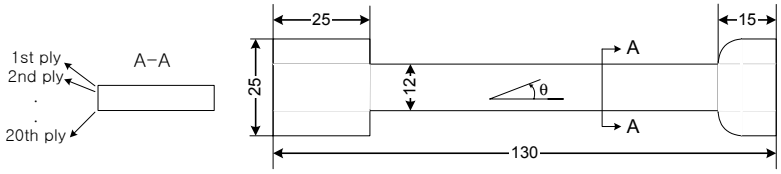

Figure 2 – Dimension of composite flexure

Table 1 – Sectional stiffness of flexures

	S_{UU} (N)	S_{TU} (N-m)	S_{WU} (N-m)	S_{VU} (N-m)	S_{TT} (N-m^2)	S_{WT} (N-m^2)	S_{VT} (N-m^2)	S_{WW} (N-m^2)	S_{VW} (N-m^2)	S_{VV} (N-m^2)
A1	1.081E+6	-6.780E+0	-3.678E+0	5.654E-1	1.178E+0	4.895E-1	-3.966E-2	4.928E-1	-2.145E-2	1.298E+1
A2	1.081E+6	6.780E+0	-3.678E+0	5.654E-1	1.178E+0	-4.895E-1	3.966E-2	4.928E-1	-2.145E-2	1.298E+1
A4	3.936E+5	-6.418E+0	-3.468E+0	5.127E-1	1.181E+0	4.917E-1	-3.830E-2	4.758E-1	-2.070E-2	4.726E+0
A6	1.607E+6	1.772E-1	-1.846E+0	6.564E-1	1.054E+0	-1.895E-2	1.292E-3	1.099E+0	-1.345E-2	1.925E+1

* A1: $[-45_8/0_2]_S$, A2: $[+45_8/0_2]_S$, A4: $[-45]_{20T}$, A6: $[0/\pm45/90_2/\mp45/0_2/90]_S$

Rotor Blade

The blade used in the present study has paddle shape as shown in *Figure 3*. The initial design of the blade was started from 1/6 scaled data from the full scale Super Lynx. And the new airfoil designed by Korea Aerospace Research Institute was applied this

blade maintaining 1/6 scale factors. The radius of full scale rotor is 6.4 m and scaled rotor system has 1.066 m radius. The solidity ratio of the rotor system is 0.0786 and the blade design and aeroelastic analysis and tests data for several similar small scaled rotor models can be found in ref. 10. The sectional analysis is of the blade has been performed using in-house code and the only isotropic terms are used.

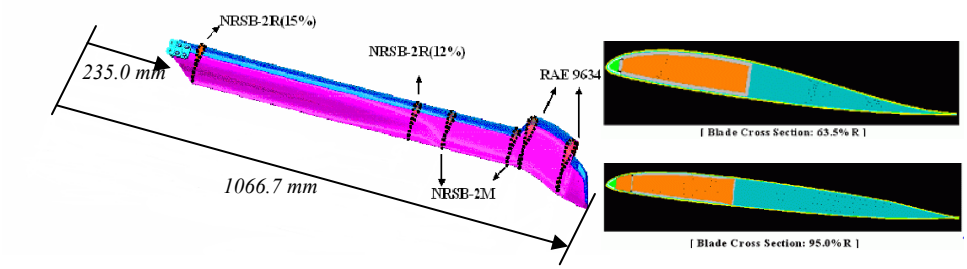

Figure 3 – Configuration of the blade

AEROELASTIC ANALYSIS OF THE ROTOR STSTEM

Aeroelastic Stability Analysis

For structural dynamic and aeroelastic stability analysis of the hingeless rotor system, commercial rotorcraft analysis code, CAMRAD II was used. The focus of this study is the investigation of the effects of coupling stiffness of the flexure. So, anisotropic model for the flexure and isotropic model for the blade has been used because the elastic deformation of the flexure is dominant. For a soft in-plane hingeless rotor system, in-plane damping is used as criterion of aeroelastic stability. Out of plane and feathering modes have high damping capacity in general. The isolated rotor system has been analyzed with rotating speed of 780 rpm and collective pitch angle -4° ~ 10°.

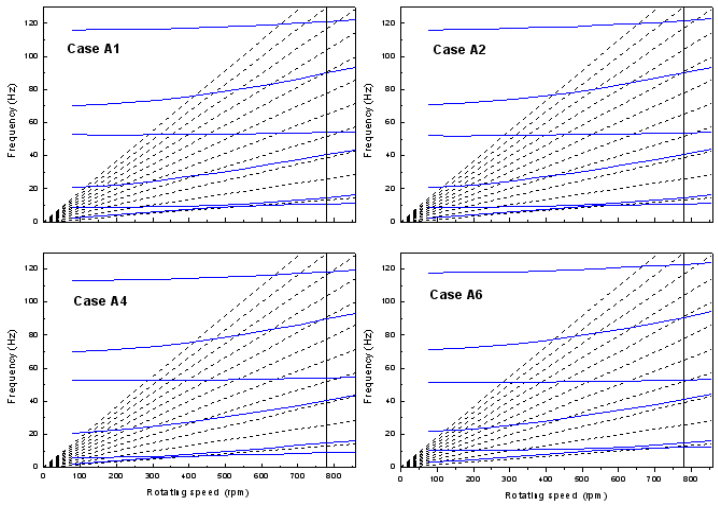

Figure 4 – Fan plots of 4 cases

The rotating frequencies of 4 different flexure cases are presented in *Figure 4*. Results of A1 and A2 are similar and A4 has slightly low and A6 has slightly high fundamental frequencies due to their stiffness. The frequency distribution does not show remarkable differences. However, the in-plane damping values are quite different for 4 cases as shown in *Figure 5*. Especially, A1 show much higher damping than A2 which has the same isotropic stiffness and similar frequency distribution.

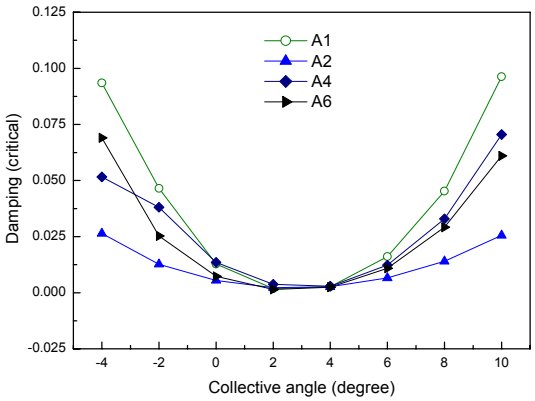

Figure 5 – In-plane damping ratios according to collective pitch angle

Effects of Coupling Stiffness

As shown in *Figure 5*, the aeroelastic stability of the rotor system can be affected by coupling stiffness. Comparing 10 independent sectional stiffness values of A1 and A2 in Table 1, just S_{TU}, S_{WT}, and S_{VT} have opposite sign, that is, A1 and A2 have contrary coupling effects related to torsional motion. The effect of individual coupling stiffness on the aeroelastic stability are calculated and compared in *Figure 6*.

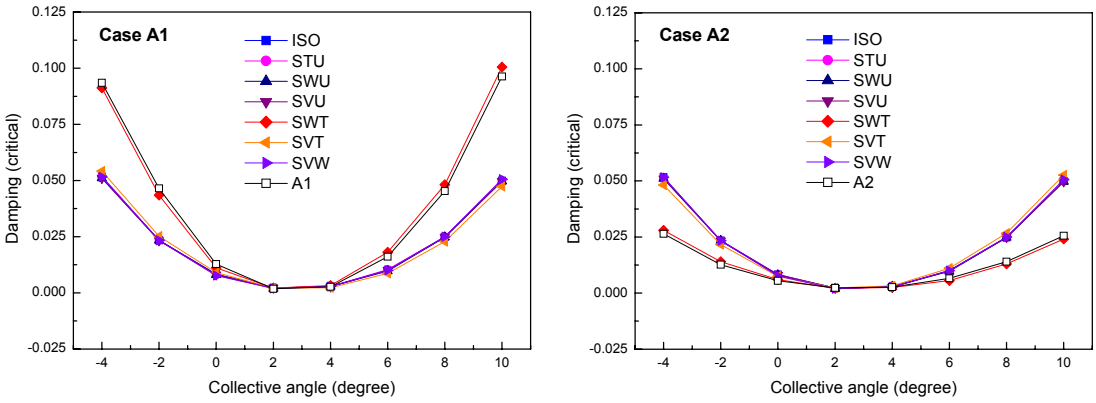

(a) case A1 *(b) case A2*

Figure 6 – Effects on coupling stiffness on in-plane damping

ISO means isotropic case, that is, only S_{UU}, S_{TT}, S_{WW}, and S_{VV} are used, and A1 and A2 are 10 stiffness values are entirely used results, and the others are results for just one coupling stiffness value denoted in the legend is used. ISO result of A1 is identical to that of A2 because S_{UU}, S_{TT}, S_{WW}, and S_{VV} are equal. We can see that S_{WT} demonstrate its effects on the in-plane damping of the rotor system. The coupled motion due to S_{WT}, torsion/flap bending coupling, can be illustrated as *Figure 7*; the same flapping motion can induce opposite feathering motion.

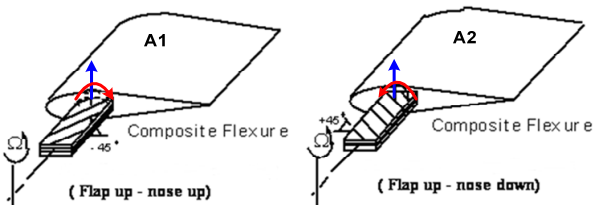

Figure 7 – Torsion-flap bending coupling

AEROELASTIC STABILITY TEST

The aeroelastic stability test of a rotor system is the investigation of the dynamic response to perturbation; in-plane damping is the object of observation. Strain gauges were constructed in full-bridge to measure flap, lag and pitch motions. In rotating condition, cyclic pitch motion was excited through nonrotating swash plate by hydraulic actuator in order to introduce lead-lag motion. In all cases, regressing mode frequency was used as excitation frequency. After a few seconds of excitation, free vibration signal was acquired, and frequency and damping were calculated using moving block method. Aeroelastic stability test were performed at general small-scaled rotor test system as shown in *Figure 8*.

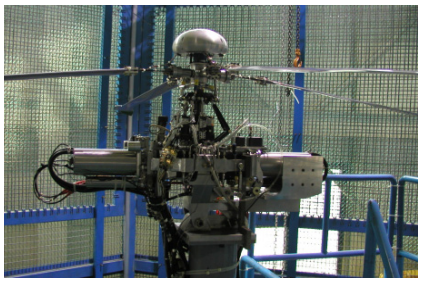

Figure 8 – General small-scaled rotor test system

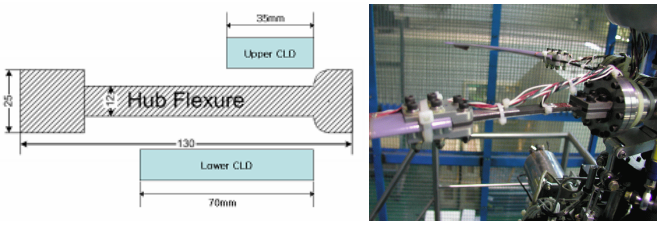

Figure 9 – Constrained layer damping treatment on the flexure

Rotating test for case A6 has been performed at 624 rpm, the other cases are under investigation, so the rotating test for the other cases are not presented in this paper. In addition to composite tailoring technique, another passive damping enhancement method has also been examined. The constrained layer damping treatment, *Figure 9*, is applied to A6 case, the test results for A6 and A6 with CLD are presented in *Figure 10*. In-plane damping of A6 is increased by about 0.01 when the CLD is applied. The

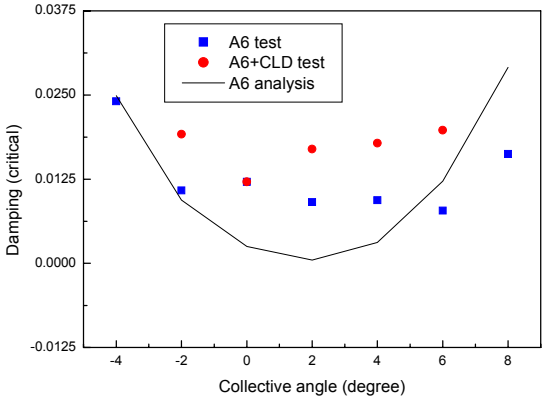

Figure 10 – Rotating test results

torsion/flap coupling and constrained layer damping treatment could be practically used in the various dynamic systems effectively. The composite tailoring technique will be utilized for developing a new kind of rotor system; it will include passive and active technologies altogether.

SUMMARY

Composite tailoring technique has been applied to flexures of a small-scaled hingeless rotor system. The effects of coupling stiffness of composite flexures on the aeroelastic stability of a small-scaled rotor system have been investigated by analysis using CAMRAD II. Among several coupling stiffness terms, torsion/flap bending coupling, S_{WT}, showed dominant influence on the in-plane damping of the rotor system. If we neglect coupling stiffness analytic or experimental result may not present actual system characteristics. In addition to composite tailoring method, viscoelastic material could be used to enhance aeroelastic stability more. These passive damping enhancement approaches could be practically used in the various actual structural systems.

REFERENCES

[1] A. Badre-Alam, K. W. Wang, and F. Gandhi, "Optimization of enhanced active constrained layer (EACL) treatment on helicopter flexbeams for aeromechanical stability augmentation," *Smart Materials and Structures*, **8**, 182-196 (1999)

[2] N. A. Koratkar and I. Chopra, "Wind tunnel testing of a Mach-scaled rotor model with trailing-edge flaps," *Smart Materials and Structures*, **10**, 1-14 (2001)

[3] M. L. Wilbur, P. H. Mirick, W. T. Yeager, C. W. Langston, C. E. S. Cesnik, and S.-J. Shin, "Vibratory Loads Reduction Testing of the NASA/Army/MIT Active Twist Rotor," *J. of the American Helicopter Society*, **47**, 123-133 (2002)

[4] W. H. Weller, "Fuselage state feedback for aeromechanical stability augmentation of a bearingless rotor", *J. of the American Helicopter Society*, **41**, 85-93. (1996)

[5] G. Kamath, N. Wereley, and M. Jolly, "Analysis and Testing of a Model-Scale Magnetorheological Fluid Helicopter Lag Mode Damper," *53rd American Helicopter Society Annual Forum*, 1325-1335 (1997)

[6] K.-D. Cho, J.-H. Han, and I. Lee, "Vibration and Damping Analysis of Laminated Plates with Fully and Partially Covered Damping Layers," *J. of Reinforced Plastics and Composites*, **19**, 1176-1200 (2000)

[7] A. R. Atilgan and D. H. Hodges, "Unified Nonlinear Analysis for Nonhomogeneous Aniso- tropic Beams with Closed Sections," *AIAA J.*, **29**, 1990-1999 (1991)

[8] A. Giavotto, M. Borri, P. Mantegazza, and G. Ghiringhelli, "Anisotropic Beam Theory and Applications," *Computers and Structures*, **16**, 403-413 (1983)

[9] W. Johnson, "Rotorcraft Dynamics Models for a Comprehensive Analysis," *AHS 54th Annual Forum*, Washington, DC, May 20-22, 1998.

[10] D.-G. Kim, J.-H. Kim, K.-W. Song, Y.-J. Kee, and G. Joo, "A Study on Aeroelastic Stability Improvement of Hingeless Hub Systems in Hover and Forward Flight Using Composite Materials," *31st European Rotorcraft Forum*, Florence, Italy, 2005